Testing the Renormalization of the von Klitzing Constant by Cavity Vacuum Fields

Josefine Enkner,[1,2,*,†] Lorenzo Graziotto,[1,2,*,‡] Felice Appugliese,[1,2] Vasil Rokaj,[3,4] Jie Wang,[5] Michael Ruggenthaler,[6] Christian Reichl,[7] Werner Wegscheider,[7] Angel Rubio,[6,8] and Jérôme Faist[1,2]

[1]*Institute of Quantum Electronics, ETH Zürich, Zürich 8093, Switzerland*
[2]*Quantum Center, ETH Zürich, Zürich 8093, Switzerland*
[3]*ITAMP, Center for Astrophysics | Harvard & Smithsonian, Cambridge, Massachusetts 02138, USA*
[4]*Department of Physics, Harvard University, Cambridge, Massachusetts 02138, USA*
[5]*Department of Physics, Temple University, Philadelphia, Pennsylvania 19122, USA*
[6]*Max Planck Institute for the Structure and Dynamics of Matter, Hamburg 22761, Germany*
[7]*Laboratory for Solid State Physics, ETH Zürich, Zürich 8093, Switzerland*
[8]*Center for Computational Quantum Physics, Flatiron Institute, New York, New York 10010, USA*

(Received 21 November 2023; accepted 2 May 2024; published 5 June 2024)

The value of fundamental physical constants is affected by the coupling of matter to the electromagnetic vacuum state, as predicted and explained by quantum electrodynamics. In this work, we present a millikelvin magnetotransport experiment in the quantum Hall regime that assesses the possibility of the von Klitzing constant being modified by strong cavity vacuum fields. By employing a Wheatstone bridge, we measure the difference between the quantized Hall resistance of a cavity-embedded Hall bar and the resistance standard, achieving an accuracy down to one part in 10^5 for the lowest Landau level. While our results do not suggest any deviation that could imply a modified Hall resistance, our work represents pioneering efforts in exploring the fundamental implications of vacuum fields in solid-state systems.

DOI: 10.1103/PhysRevX.14.021038

Subject Areas: Condensed Matter Physics, Optoelectronics

I. INTRODUCTION

In condensed-matter physics, the vacuum fields refer to the quantum fluctuations of the ground-state electromagnetic field, which owing to Heisenberg's uncertainty principle, possess zero average but finite variance [1]. Although energy conservation prevents the direct probing of their virtual excitations, vacuum fields manifest their physical reality via the interaction with matter systems, leading to experimentally accessible modifications of their energy spectra, such as the Lamb shift [2], or fundamental properties, such as the electron magnetic moment [3]. Both effects are very well understood within quantum electrodynamics (QED) [4,5]. In recent years, the possibility of shaping the vacuum fields inside cavities has been proposed [6,7] as a means of engineering matter properties, such as the electron-phonon coupling [8] and the molecular structure [9], altering matter phases, such as superconductivity [10] and ferroelectricity [11], or affecting nonequilibrium phenomena like chemical reactions [12] and charge transport [13]. Experimental progress has been made particularly in showing the cavity-altered ground-state chemical reactivity [14,15], and recently we experimentally showed how cavity vacuum fields can destroy the topological protection of the integer quantum Hall states [16]. The breakdown manifests in the cavity-induced backscattering of the otherwise zero-resistance edge states, which yields a finite longitudinal resistivity accompanied by a loss of quantization of the transverse (Hall) resistivity. The backscattering mechanism, which is attributed to a cavity-assisted hopping term in the Hamiltonian [17], affects, in particular, edge states at high odd integer filling factors $\nu = n_s h/eB$, where n_s indicates the two-dimensional (2D) electron density, h is Planck's constant, e the electron charge, and B the magnetic flux density in the direction orthogonal to the 2D electron system (2DES).

Quantum Hall states at high filling factor, i.e., at low magnetic field, are more prone to be affected by cavity vacuum fields since the extent of the electronic wave functions scales with the square of the magnetic length $l_B = \sqrt{\hbar/eB}$; thus, at lower magnetic fields it will be easier for the cavity-induced hopping to couple states which are more spatially overlapped. Equivalently, the energy gap in the Landau-level density of states scales

*These authors contributed equally to this work.
†enknerj@phys.ethz.ch
‡lgraziotto@phys.ethz.ch

with B; hence, at lower B the edge states will be energetically closer to the disordered bulk states into which, according to the picture developed in Ref. [17], they are eventually scattered. This is particularly the case for odd integer filling factors, which involve spin-resolved Landau levels separated by the Zeeman energy splitting, which is generally lower than the cyclotron gap.

Increasing the magnetic field, i.e., going to lower integer filling factors, quantization is indeed fully recovered (as evident when looking at the data of Ref. [16] in the high-magnetic-field region $B > 3$ T), with the longitudinal resistivity going to zero and the Hall resistivity developing plateaux. In 2D electron systems not embedded in cavity vacuum fields, the value of these plateaux is given by reciprocal-integer multiples of von Klitzing's constant $R_K = h/e^2$, the equality being supported by theoretical gauge [18,19] and topological [20,21] arguments, and experimentally verified down to eight parts in 10^{11} [22]. For this reason, the integer quantum Hall effect (IQHE) [23] remains essential in the foundation of the standard electrical resistance even after the changes in the International System of Units [24,25]. On the other hand, a precise measurement of the quantized values of the Hall plateaux for 2D electron systems embedded in cavities has not yet been performed, and one may inquire if these values show deviations from the value of R_K, that is if cavity vacuum fields can modify the value of R_K. Indeed, a tiny 10^{-20} correction due to the coupling to the free-electromagnetic field was already calculated within QED [26], and given the recent advances in the engineering of electromagnetic environments which can nonperturbatively couple to Landau electrons [27–30], it is reasonable not only to investigate if a modification arises in such conditions, but also to employ a simple and controlled experimental platform like the 2DES to gain general physical insights into vacuum-induced phenomena in condensed-matter systems.

Although they share a common origin in the vacuum fluctuations, we remark that the hypothetical modification of R_K, which we aim to test in the present work, is markedly different from the vacuum-induced scattering reported in Ref. [16]. The distinction is clear both in the measurement scheme and in the physical mechanism which is investigated. As discussed above, the experiment of Ref. [16] deals with edge states at high integer filling factors, and shows how vacuum fields act as a source of finite longitudinal resistivity; i.e., edge states are no more immune to backscattering [31]. In contrast, the present work deals with fully quantized states—with zero longitudinal resistivity—at low integer filling factors, and assesses if the quantized transverse resistivity shows deviations from the value obtained without considering any impact of the cavity electromagnetic field. High accuracy is achieved only for low enough filling factors, since it is necessary to take averages of the transverse resistivity over Hall plateaux which extend over a wide magnetic field range. Furthermore, as is addressed below, in the present work the placement of the electrical contacts is different from the one of Ref. [16], being aimed at probing a different phenomenon. Nevertheless, as we discuss at the end, we can observe an effect of the cavity on the quantization accuracy by means of a temperature study.

Recently, it has been theoretically predicted [32] via a simplified approach that the quantized Hall resistance of a cavity-embedded 2D electron system should display a deviation from R_K proportional to the square of the light-matter coupling. The result is obtained under the assumptions that the 2DES is infinite and homogeneous and that the single-mode cavity frequency ω_{cav} is much smaller than any other energy scale involved (and thus the limit of zero cavity frequency is taken). Under these assumptions, and disregarding electron-electron interactions which do not play a role in the IQHE, the theory predicts that the plateau of filling factor ν should possess a quantized value $R_H = R_K \nu^{-1}(1+\eta^2)$. Being the cavity frequency negligible, the dimensionless collective light-matter coupling is more properly quantified via the ratio $\eta = \omega_d/\omega_{\mathrm{cyc}}$ of the diamagnetic frequency, which originates [33] from the squared cavity vector potential $\hat{\mathbf{A}}^2$ (and its definition is reported in Sec. V of the Supplemental Material [34]) to the cyclotron frequency, as opposed to the customary definition via the ratio $\chi = g/\omega_{\mathrm{cyc}}$, where g is the collective vacuum Rabi frequency defined as Ω in Ref. [33]. Via the Thomas-Reiche-Kuhn sum rule, one can prove [35] that $\omega_d = 2g\sqrt{\omega_{\mathrm{cav}}/\omega_{\mathrm{cyc}}}$; indeed, in the ultrastrong-coupling regime the diamagnetic term in the Hamiltonian is not negligible. In this work, we show experimentally that cavity vacuum fields bear no impact on the value of the quantized Hall resistance down to one part in 10^5 for $\nu = 1$, hence setting a clear limit on the validity of the theoretical assumptions.

II. RESULTS

The geometry of the experiment is centered on a 40-μm-wide Hall bar placed in the capacitor gap of a complementary split-ring resonator (CSRR) [36] resonant at $\omega_{\mathrm{cav}} = 2\pi \times 140$ GHz, which we refer to as the cavity in the following [see Fig. 1(a), where the cavity-embedded Hall bar is labeled by number 4]. CSRRs have the ability to strongly enhance vacuum fields $\mathcal{E} = \sqrt{\hbar\omega_{\mathrm{cav}}/2\epsilon_0\epsilon_s V_{\mathrm{eff}}}$ in a subwavelength volume $V_{\mathrm{eff}} = 2.7 \times 10^5$ μm^3, ϵ_0 being the vacuum permittivity, and $\epsilon_s = 12.69$ the effective permittivity of GaAs, the material in which the 2D electron system is hosted (more details are provided in the Supplemental Material [34]). As a result, the interaction between enhanced cavity vacuum fields and the electrons occupying the last filled Landau level is pushed into the ultrastrong-coupling regime [35], leading to a normalized coupling $\tilde{g}/\omega_{\mathrm{cav}} \approx 0.3$, where $\tilde{g}$ is the collective vacuum

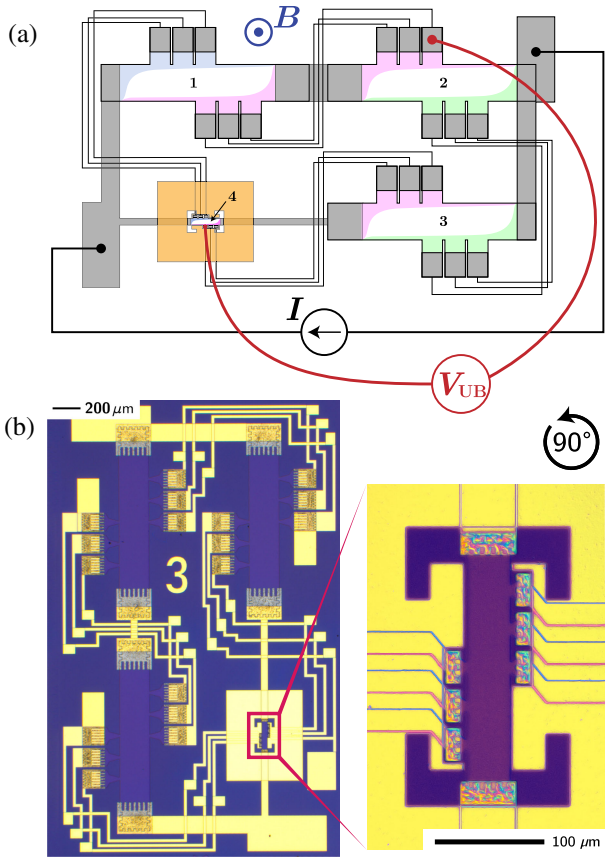

FIG. 1. Layout of the sample. (a) Sketch of cavity sample S3, where the measurement scheme is illustrated. The current I is injected and extracted from the source-drain contacts, and the unbalance voltage V_{UB} is measured at the indicated voltage probes. The gray color indicates metal contacts and leads. The pale color shadings indicate regions having the same electric potential, in the situation in which the cavity does not alter the value of the quantized Hall resistance, so that the same current circulates in each arm of the Wheatstone bridge. The thin black lines indicate additional gold leads which connect contacts on regions of the Hall bars having the same electric potential, in order to ensure their equilibration. (b) Microscope picture of cavity sample S3, with cavity-embedded Hall bar on the lower right, which is enlarged on the right. Notice that the picture is rotated by 90° counterclockwise with respect to (a).

Rabi frequency g at zero detuning (i.e., when $\omega_{cav} = \omega_{cyc}$). We point out that in the experiment, the Hall bar, together with the contacts to the 2D electron system, is completely inside the spatial gap of the cavity (at variance with the experiment of Ref. [16]), as can be seen in Fig. 1(b), where a microscope picture of the sample and an enlargement of the cavity-embedded Hall bar are shown. The design reason follows from the following argument [37]: All systems which are adiabatically connected (i.e., by varying some external parameters, they can be transformed into one another without closing their spectral gap) to any system exhibiting a topological invariant must then also—at zero temperature—have that same topological invariant. The quantized transverse resistivity R_K/ν is a topological invariant for the IQHE. Since the predicted modification of the transverse resistivity due to cavity vacuum fields is not necessarily topological in nature, putting the whole Hall bar structure, together with its contacts, inside the cavity prevents the system from relapsing into its exactly quantized state at the contacts lying outside of the cavity. At the same time, two gapped systems with different Hall resistivities must have a gap closing between them, a requirement which is fulfilled via the metal contacts connecting the Hall bars both in series and in parallel. Again, even if the deviation from the quantized value introduced by cavity vacuum fields in the Hall bar is not a topological invariant, we can preserve and access it experimentally. Finally, placing the contacts inside the Hall bar has the side effect of reducing the scattering processes arising due to the vacuum field gradients at the boundary between the cavity capacitor gap and the etched lateral sides of the Hall bar. These field gradients amplify the effect that backscatters the edge states, which is not what we are investigating in the present work, since we want to preserve the quantization of the Hall resistance, and assess whether the quantization value is changed.

To highlight deviations in standard Hall quantization compared to a Hall bar in the presence of cavity vacuum fields, we arrange three 200-μm-wide bare Hall bars [i.e., not embedded in a cavity; see Fig. 1(a), where they are labeled by numbers 1–3] and the aforementioned 40-μm-wide cavity-embedded Hall bar (number 4) in a Wheatstone bridge configuration [22]. This allows for the measurement of unknown resistances by detecting the unbalance voltage V_{UB} at the junction between the two resistors of each arm [see Fig. 1(a)]. By using three bare Hall bars as reference resistors, we take advantage of the fact that at the plateaux they possess the same resistance R_K/ν, while the deviation of the cavity-embedded Hall bar resistance from the quantized value will be proportional to the unbalance voltage via

$$\frac{\Delta R_H}{R_H} = 4\frac{\langle V_{UB}\rangle}{I}\frac{e^2}{h}\nu, \tag{1}$$

where $I = 10$ nA is the source-drain current that flows in the Wheatstone bridge, and $\langle V_{UB}\rangle$ is the unbalance voltage averaged at the integer plateau ν [a derivation of Eq. (1) is given in Sec. I of the Supplemental Material [34]]. The low injection current is in contrast to standard metrological measurement methods, since here we aim at achieving very low base temperatures in order to stay as close as possible to the regime for which the renormalization is predicted (close to $T = 0$) [32]. At the plateaux, in the case in which no deviation due to cavity vacuum fields occurs, the voltage drop across both resistors in each arm will be the same; thus, the unbalance voltage will be zero [see Fig. 1(a), where the pale color shadings indicate regions with equal

electric potential in the case of no deviation]. The finite contact resistance R_C of the metallic contacts to the 2DES could hinder the measurement of V_{UB}; hence, the quadruple connection technique is employed [38]. This technique involves introducing additional connections between pairs of Hall bars [shown by the three thin black lines in Fig. 1(a), in addition to the connection via the leads depicted in gray], each possessing a resistance R_C, which bridge the equipotential sides of the Hall bars. We therefore ensure the equilibration of the equipotential sides as the relative contribution of the contact resistance of each Ohmic contact is reduced to a factor of $(R_C/R_H)^4$ (i.e., to about 1.4×10^{-7} for filling factor 1). To assess potential variations in the measurement result coming from sample-specific properties (due, e.g., to inhomogeneities in the material), we fabricate one chip comprising five samples. Three of them (labeled S3–S5) possess the cavity-embedded Hall bar resonator, as discussed above [a microscope picture of sample S3 is displayed in Fig. 1(b)]. Samples S1 and S2 have instead the same configuration but no resonator [only the bare 40-μm Hall bar indicated by number 4 in Fig. 1(a)] and serve as references. All five samples are processed from the same 2D electron system obtained in a high-mobility GaAs/AlGaAs square quantum well (see Appendix). Indeed, the impact of cavity vacuum fields on transport has been shown on high-mobility samples [16], although such high values would be in contrast to standard metrological techniques. Fabrication is performed via standard photolithography, with an intermediate step where we deposit an insulating layer of Al_2O_3 that electrically separates the overlapping gold planes and lines from each other. Vias in the insulating layer are opened with hydrofluoric acid etching in order to achieve the quadruple connection scheme.

In Fig. 2, we display the unbalance voltage evolution as a function of the perpendicular magnetic field B for a reference (S1) and for a cavity (S3) sample at an electronic temperature below 20 mK. We remind that a meaningful comparison between the two can be performed only at the plateaux, since away from them the three reference Hall bars have not a quantized resistance, and the unbalance voltage is mostly determined by the material inhomogeneities over the sample area. Enlarging the plateaux regions (insets of Fig. 2), we observe that both reference and cavity traces oscillate around zero, within a range of ± 2 nV. The main contribution to the noise comes from the ac preamplifier voltage noise, which for a demodulation frequency of 2.333 Hz amounts to about 2.6 $\mathrm{nV}/\sqrt{\mathrm{Hz}}$ (more details are given in the Appendix). The plateaux regions are identified by the filling factor ν, and for the purposes of the following analysis, their extension is determined by taking 3.2 nV as threshold value for the absolute value of V_{UB}. In Fig. 3, we report the relative deviation $\Delta R_H/R_H$ from the Hall resistance at the integer plateaux as given by Eq. (1), where we estimate the unbalance voltage as a weighted average for both reference and cavity samples. Indeed, the main source of uncertainty

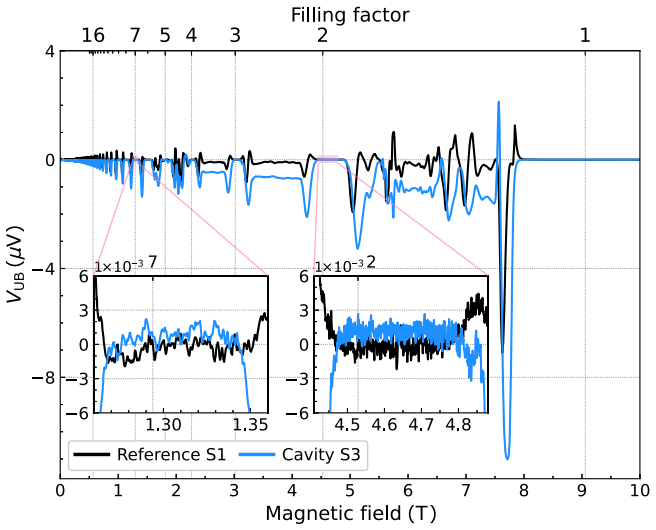

FIG. 2. Measurement of the unbalance voltage of the Wheatstone bridge as a function of the magnetic field for nominal value of the current injected $I = 10$ nA, in the case of a sample without the cavity (black curve, S1) and with the cavity (blue curve, S3). The insets show an enlargement near the plateaux $\nu = 7$ and $\nu = 2$. Notice that the vertical axis values of the insets are multiplied by 10^3.

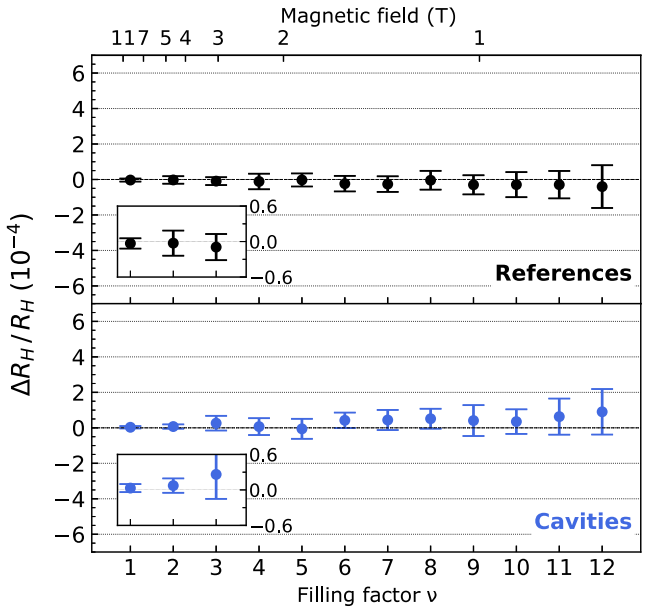

FIG. 3. Weighted averages of the relative deviation from the Hall resistance as a function of the integer filling factor, for samples without the cavity (top panel) and with the cavity (bottom panel). The error bars indicate a 99.7% confidence interval of the values at the plateaux (i.e., 3 standard deviations). The relative deviation is below one part in 10^5 for $\nu = 1$, as can be seen in the insets, where the region between $\nu = 1$ and $\nu = 3$ is enlarged, and it is below 1×10^{-4} for $\nu = 12$.

is statistical for $\nu > 2$, while for $\nu \leq 2$ sample-specific uncertainties dominate, and we assess them by measuring multiple reference and cavity samples (a more detailed discussion about the nature of the uncertainties is given in Sec. III of the Supplemental Material [34]). The error bars display a 99.7% confidence interval (i.e., their length is equal to 3 standard deviations) of the data distribution at each plateau. We notice that both the cavity and the reference samples show a deviation from the quantized Hall resistance compatible with zero within this confidence interval.

Hence, we reject the possibility of a relative deviation from the quantized value of the plateaux larger than 3 standard deviations, that is, below 1×10^{-5} for $\nu = 1$ and below 2×10^{-4} for $\nu = 12$. For higher filling factors (that is, lower magnetic fields), the relative uncertainty is larger due to the smaller Hall resistance and the smaller extension of the plateaux. Although the precision we achieve is far from the one reported in Ref. [22], it constitutes an upper bound to the effect that cavity vacuum fields may bear on the value of R_K. This result may be compared to the ratio of the Lamb shift to the Dirac levels of the hydrogen atom, which amounts to about 4×10^{-7}, and which quantifies the relative correction introduced by free vacuum fields to the energy levels uncoupled from the electromagnetic field, or to the relative contribution of about 10^{-3} of the radiative corrections on the magnetic moment of the electron [1], or also to the small 10^{-20} free-field radiative correction to R_K predicted in Ref. [26] within QED.

III. DISCUSSION AND CONCLUSION

We can now address the incompatibility of the experimental result with the theoretical prediction of Ref. [32]. As discussed above, therein a renormalized value was found in the limit of zero temperature and assuming that the cavity frequency is so small that it can be neglected and taken to zero. However, the latter assumption is too crude for the system under study, which possesses, due to the lateral confinement of the etched Hall bar, a minimum energy scale given by the plasma frequency $\omega_p \simeq 2\pi \times 90$ GHz (for the 40-μm-wide Hall bar), which corresponds to the longitudinal collective excitation of the free-electron gas. This frequency sets a fundamental lower limit for achieving light-matter hybridization [39], and indeed our choice of $\omega_{\mathrm{cav}} = 2\pi \times 140\ \mathrm{GHz} > \omega_p$ was motivated by this constraint. Theoretically, as shown in the Supplemental Material [34], one can avoid setting the cavity frequency to zero and still preserve the assumption of homogeneity with an approach based on the Kubo formalism [40,41], which shows indeed that for low enough temperatures (i.e., below the excitation energy of the light-matter hybrid states), one recovers the exact quantization of the Hall resistivity even when cavity vacuum fields are present. If the cavity frequency is considered to be negligible as compared to the other energy scales in the system, the lower polariton mode goes to zero (see also Sec. V of the Supplemental Material [34]). This is a singular point for the system because the lower polariton gap closes, and thus circumvents the Thouless flux insertion argument which assumes a finite gap [21]. The gap closing would lead to the deviation of the Hall resistivity from the precise quantization $R_H = R_K/\nu$ [32]. Finally, one may inquire whether the cavity has an impact on the quantization accuracy through a thermally activated deviation [42,43], as was predicted in Ref. [41]. In Sec. IV of the Supplemental Material [34], we provide data as a function of the temperature, which indeed show a reduced activation energy for the cavity samples as compared to the reference ones, in the same fashion as shown in the Supplemental Material of Ref. [16]. Further investigation is needed to explain this behavior through the framework developed in Ref. [41].

The present work serves as a foundation for investigating the effect of cavity vacuum fields on fundamental constants in solid-state systems. Using the 2DES as the simplest solid-state experimental platform, and measuring the impact of cavity vacuum fields on the Hall resistance employing the high-accuracy Wheatstone bridge measurement technique, we have assessed that no deviation from von Kliting's constant is present up to one part in 10^5 for filling factor 1. We believe that at this stage the accuracy is mainly limited by electron-density inhomogeneities present across the sample. In a more advanced version of this experiment, a further increase in precision can be achieved by injecting direct current, or by employing a cryogenic current comparator, hence investigating whether the deviation is smaller in magnitude, or if it can arise due to finite-temperature effects [41]. The proposed experimental platform could also be employed to study the impact of cavity vacuum fields on electron systems hosted in other different two-dimensional materials.

ACKNOWLEDGMENTS

We thank Giacomo Scalari for useful discussions and Peter Märki for technical support. We acknowledge funding from the Swiss National Science Foundation through Grant No. 200020-207795. V. R. acknowledges support from the U.S. National Science Foundation through a grant for ITAMP at Harvard University. J. F. thanks the Alexander von Humboldt Foundation for their support.

APPENDIX: MATERIALS AND METHODS

The 2DES is obtained in a GaAs/AlGaAs quantum well grown via molecular-beam epitaxy. The quantum well is 30 nm wide and modulation doped, with a 100-nm spacer. The electron density and mobility measured at 1.3 K in the dark are $n_s = 2.06 \times 10^{11}\ \mathrm{cm}^{-2}$ and $\mu = 1.59 \times 10^7\ \mathrm{cm}^2\,\mathrm{V}^{-1}\,\mathrm{s}^{-1}$, respectively. At mK temperatures from the location of the integer filling factor plateaux,

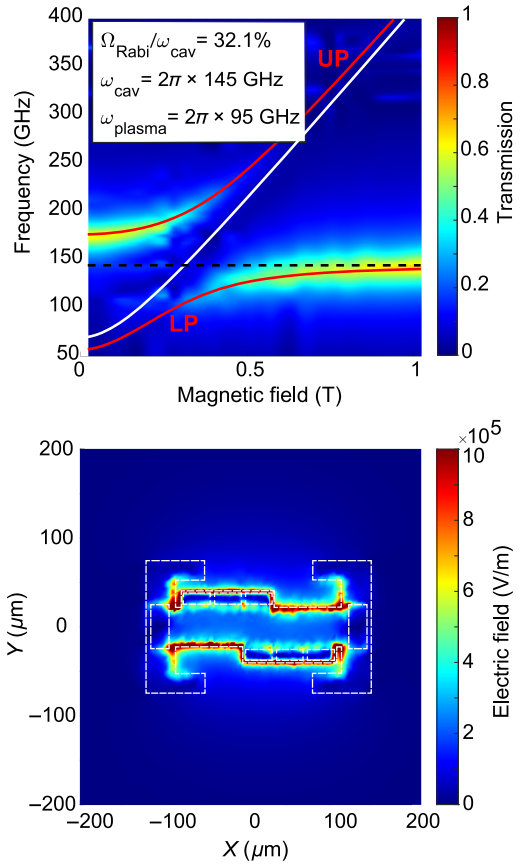

FIG. 4. Results from the finite-element simulations. Top: color plot of the transmission of the coupled structure as a function of the magnetic field and frequency. Because of the ultrastrong light-matter coupled nature of the system, the transmission spectrum follows a polaritonic dispersion, with distinguishable upper (UP) and lower (LP) polaritons. Bottom: color map of the absolute value of the in-plane electric field in the cavity structure. Outlines of the cavity structure are drawn in white [compare with Fig. 1(b)].

we extract a density $n_s = 2.2 \times 10^{11}$ to 2.4×10^{11} cm^{-2}, varying between different samples. In the figures of the main text and the Supplemental Material [34], the magnetic field scale for all samples but the first reference is thus stretched to align the plateaux according to the different densities. The samples are processed via standard photolithography techniques in a clean-room environment.

The cavity consists of a CSRR, and it is designed to have its fundamental mode at 145 GHz. The normalized coupling strength between the cavity vacuum field and the 2DES depends on the effective cavity volume and the electron density as $\tilde{g}/\omega_{\mathrm{cav}} \propto \sqrt{n_s/V_{\mathrm{eff}}}$. To assess the coupling dynamics of the system, finite-element simulations are conducted using the CST Microwave Studio software, obtaining a normalized coupling of $\tilde{g}/\omega_{\mathrm{cav}} \approx 0.3$ (see Fig. 4). The resonator is modeled using the standard gold (lossy material) sourced from the material library. The substrate is implemented as a block of GaAs. The 2DES is modeled using a gyrotropic material with bias (i.e., the magnetic field) oriented perpendicular to the surface. To mitigate computational expenses, an effective layer thickness is incorporated. Similar designs have been already implemented in previous experiments, and for a detailed examination of transmission spectra experiments describing a setup similar to the one of the present work, we direct readers to Refs. [16,44].

The experiment is conducted with state-of-the-art methods for measurement of the quantum Hall effect in two-dimensional electron systems [45]. We employ a Bluefors dilution refrigerator capable of reaching temperatures down to 10 mK. The voltage is measured with commercial MFLI Zurich Instruments digital lock-in amplifiers. Current is injected symmetrically in the Wheatstone bridge by applying an ac-modulated voltage of 2-V root-mean-square (rms) at the demodulation frequency $f_{\mathrm{dem}} = 2.333$ Hz to two 100-MΩ resistors in series with the Wheatstone bridge, such that a current of 10-nA rms is circulating in the circuit. Differential ac low-noise preamplifiers are employed before the lock-in voltage input, so to amplify the signal by a factor of 1000. The amplifier input voltage noise density amounts to $2.6\ \mathrm{nV}/\sqrt{\mathrm{Hz}}$ at the demodulation frequency f_{dem}, while the input current noise is negligible in the balanced detection scheme. Moreover, the common mode amplification does not introduce any unwanted offset, since in the balanced detection scheme with symmetric current injection the absolute voltages are close to zero. To demodulate the lock-in input signal, we employ a fourth-order low-pass filter with time constant of 1.0 s, which corresponds to a noise-equivalent-power bandwidth of 0.079 Hz, so that the input voltage noise is 0.7 nV. The input noise of the lock-in signal input is negligible with respect to the noise of the amplified signal. Before the contacts to the sample, low-pass 100-kHz filters are installed in order to minimize electric spikes or heating effects from the measurement setup.

[1] P. Milonni, *The Quantum Vacuum: An Introduction to Quantum Electrodynamics* (Elsevier Science, New York, 1994).
[2] W. Lamb and R. Retherford, *Fine structure of the hydrogen atom by a microwave method*, Phys. Rev. **72**, 241 (1947).
[3] P. Kusch and H. M. Foley, *The magnetic moment of the electron*, Phys. Rev. **74**, 250 (1948).
[4] C. Cohen-Tannoudji, J. Dupont-Roc, and G. Grynberg, *Photons and Atoms: Introduction to Quantum Electrodynamics* (Wiley, New York, 1989).
[5] M. Peskin and D. Schroeder, *An Introduction to Quantum Field Theory*, Frontiers in Physics (Addison-Wesley Publishing Company, Boston, 1995).
[6] F. Garcia-Vidal, C. Ciuti, and T. Ebbesen, *Manipulating matter by strong coupling to vacuum fields*, Science **373**, eabd0336 (2021).

[7] H. Hübener, U. De Giovannini, C. Schäfer, J. Andberger, M. Ruggenthaler, J. Faist, and A. Rubio, *Engineering quantum materials with chiral optical cavities*, Nat. Mater. **20**, 438 (2021).

[8] M. A. Sentef, M. Ruggenthaler, and A. Rubio, *Cavity quantum-electrodynamical polaritonically enhanced electron-phonon coupling and its influence on superconductivity*, Sci. Adv. **4**, eaau6969 (2018).

[9] J. Galego, F. J. Garcia-Vidal, and J. Feist, *Cavity-induced modifications of molecular structure in the strong-coupling regime*, Phys. Rev. X **5**, 041022 (2015).

[10] F. Schlawin, A. Cavalleri, and D. Jaksch, *Cavity-mediated electron-photon superconductivity*, Phys. Rev. Lett. **122**, 133602 (2019).

[11] Y. Ashida, A. Imamoğlu, J. Faist, D. Jaksch, A. Cavalleri, and E. Demler, *Quantum electrodynamic control of matter: Cavity-enhanced ferroelectric phase transition*, Phys. Rev. X **10**, 041027 (2020).

[12] R. F. Ribeiro, L. A. Martínez-Martínez, M. Du, J. Campos-Gonzalez-Angulo, and J. Yuen-Zhou, *Polariton chemistry: Controlling molecular dynamics with optical cavities*, Chem. Sci. **9**, 6325 (2018).

[13] D. Hagenmüller, J. Schachenmayer, S. Schütz, C. Genes, and G. Pupillo, *Cavity-enhanced transport of charge*, Phys. Rev. Lett. **119**, 223601 (2017).

[14] A. Thomas, J. George, A. Shalabney, M. Dryzhakov, S. J. Varma, J. Moran, T. Chervy, X. Zhong, E. Devaux, C. Genet *et al.*, *Ground-state chemical reactivity under vibrational coupling to the vacuum electromagnetic field*, Angew. Chem. **128**, 11634 (2016).

[15] W. Ahn, J. F. Triana, F. Recabal, F. Herrera, and B. S. Simpkins, *Modification of ground-state chemical reactivity via light–matter coherence in infrared cavities*, Science **380**, 1165 (2023).

[16] F. Appugliese, J. Enkner, G. Paravicini-Bagliani, M. Beck, C. Reichl, W. Wegscheider, G. Scalari, C. Ciuti, and J. Faist, *Breakdown of topological protection by cavity vacuum fields in the integer quantum Hall effect*, Science **375**, 1030 (2022).

[17] C. Ciuti, *Cavity-mediated electron hopping in disordered quantum Hall systems*, Phys. Rev. B **104**, 155307 (2021).

[18] R. B. Laughlin, *Quantized Hall conductivity in two dimensions*, Phys. Rev. B **23**, 5632 (1981).

[19] B. I. Halperin, *Quantized Hall conductance, current-carrying edge states, and the existence of extended states in a two-dimensional disordered potential*, Phys. Rev. B **25**, 2185 (1982).

[20] D. J. Thouless, M. Kohmoto, M. P. Nightingale, and M. den Nijs, *Quantized Hall conductance in a two-dimensional periodic potential*, Phys. Rev. Lett. **49**, 405 (1982).

[21] D. Thouless, *Topological interpretations of quantum Hall conductance*, J. Math. Phys. **35**, 5362 (1994).

[22] F. Schopfer and W. Poirier, *Testing universality of the quantum Hall effect by means of the Wheatstone bridge*, J. Appl. Phys. **102**, 054903 (2007).

[23] K. v. Klitzing, G. Dorda, and M. Pepper, *New method for high-accuracy determination of the fine-structure constant based on quantized Hall resistance*, Phys. Rev. Lett. **45**, 494 (1980).

[24] *Proceedings of the Comptes rendus de la 26e réunion de la CGPM (CGPM 2018)* (Bureau International des Poids et Mesures, 2018), https://www.bipm.org/documents/20126/30876792/CGPM26.pdf/9db96c32-a986-e32a-09f9-3ed7e6c77cf7.

[25] A. F. Rigosi and R. E. Elmquist, *The quantum Hall effect in the era of the new SI*, Semicond. Sci. Technol. **34**, 093004 (2019).

[26] A. A. Penin, *Quantum Hall effect in quantum electrodynamics*, Phys. Rev. B **79**, 113303 (2009).

[27] V. M. Muravev, I. V. Andreev, I. V. Kukushkin, S. Schmult, and W. Dietsche, *Observation of hybrid plasmon-photon modes in microwave transmission of coplanar microresonators*, Phys. Rev. B **83**, 075309 (2011).

[28] Q. Zhang, M. Lou, X. Li, J. L. Reno, W. Pan, J. D. Watson, M. J. Manfra, and J. Kono, *Collective non-perturbative coupling of 2d electrons with high-quality-factor terahertz cavity photons*, Nat. Phys. **12**, 1005 (2016).

[29] X. Li, M. Bamba, Q. Zhang, S. Fallahi, G. C. Gardner, W. Gao, M. Lou, K. Yoshioka, M. J. Manfra, and J. Kono, *Vacuum Bloch-Siegert shift in Landau polaritons with ultra-high cooperativity*, Nat. Photonics **12**, 324 (2018).

[30] G. L. Paravicini-Bagliani, F. Appugliese, E. Richter, F. Valmorra, J. Keller, M. Beck, N. Bartolo, C. Rössler, T. Ihn, K. Ensslin *et al.*, *Magneto-transport controlled by Landau polariton states*, Nat. Phys. **15**, 186 (2019).

[31] M. Büttiker, *Absence of backscattering in the quantum Hall effect in multiprobe conductors*, Phys. Rev. B **38**, 9375 (1988).

[32] V. Rokaj, M. Penz, M. A. Sentef, M. Ruggenthaler, and A. Rubio, *Polaritonic Hofstadter butterfly and cavity control of the quantized Hall conductance*, Phys. Rev. B **105**, 205424 (2022).

[33] D. Hagenmüller, S. De Liberato, and C. Ciuti, *Ultrastrong coupling between a cavity resonator and the cyclotron transition of a two-dimensional electron gas in the case of an integer filling factor*, Phys. Rev. B **81**, 235303 (2010).

[34] See Supplemental Material at http://link.aps.org/supplemental/10.1103/PhysRevX.14.021038 for the derivation of Eq. (1) in the main text, the unbalance voltage traces of all samples, the discussion on measurement uncertainties, the temperature study, and the theoretical background.

[35] A. Frisk Kockum, A. Miranowicz, S. De Liberato, S. Savasta, and F. Nori, *Ultrastrong coupling between light and matter*, Nat. Rev. Phys. **1**, 19 (2019).

[36] G. Scalari, C. Maissen, D. Turčinková, D. Hagenmüller, S. De Liberato, C. Ciuti, C. Reichl, D. Schuh, W. Wegscheider, M. Beck *et al.*, *Ultrastrong coupling of the cyclotron transition of a 2d electron gas to a THz metamaterial*, Science **335**, 1323 (2012).

[37] R. B. Laughlin, *Nobel lecture: Fractional quantization*, Rev. Mod. Phys. **71**, 863 (1999).

[38] F. Delahaye, *Series and parallel connection of multiterminal quantum Hall-effect devices*, J. Appl. Phys. **73**, 7914 (1993).

[39] S. Rajabali, E. Cortese, M. Beck, S. De Liberato, J. Faist, and G. Scalari, *Polaritonic nonlocality in light–matter interaction*, Nat. Photonics **15**, 690 (2021).

[40] N. Bartolo and C. Ciuti, *Vacuum-dressed cavity magnetotransport of a two-dimensional electron gas*, Phys. Rev. B **98**, 205301 (2018).

[41] V. Rokaj, J. Wang, J. Sous, M. Penz, M. Ruggenthaler, and A. Rubio, *Weakened topological protection of the quantum Hall effect in a cavity*, Phys. Rev. Lett. **131**, 196602 (2023).

[42] M. Fogler and B. Shklovskii, *Thermally activated deviations from quantum Hall plateaux*, Solid State Commun. **94**, 503 (1995).

[43] J. Matthews and M. Cage, *Temperature dependence of the Hall and longitudinal resistances in a quantum Hall resistance standard*, J. Res. Natl. Inst. Stand. Technol. **110**, 497 (2005).

[44] G. L. Paravicini-Bagliani, G. Scalari, F. Valmorra, J. Keller, C. Maissen, M. Beck, and J. Faist, *Gate and magnetic field tunable ultrastrong coupling between a magnetoplasmon and the optical mode of an LC cavity*, Phys. Rev. B **95**, 205304 (2017).

[45] S. Baer and K. Ensslin, *Transport Spectroscopy of Confined Fractional Quantum Hall Systems* (Springer, New York, 2015), Vol. 183.